Title

Release and detection of nanosized copper from a commercial antifouling paint.

Authors

Adeleye, Adeyemi S

Oranu, Ekene A

Tao, Mengya

et al.

Publication Date

2016-10-01

DOI

10.1016/j.watres.2016.06.056

Peer reviewed

Water Research 102 (2016) 374–382

Contents lists available at ScienceDirect

Water Research

journal homepage: www.elsevier.com/locate/watres

Release and detection of nanosized copper from a commercial antifouling paint

Adeyemi S. Adeleye [a, c], Ekene A. Oranu [b, c], Mengya Tao [a], Arturo A. Keller [a, c, *]

[a] Bren School of Environmental Science & Management, University of California, Santa Barbara, CA 93106-5131, USA
[b] College of Letters & Science, University of California, Santa Barbara, CA 93106-5131, USA
[c] University of California Center for Environmental Implications of Nanotechnology, Santa Barbara, CA, USA

ARTICLE INFO

Article history:
Received 20 April 2016
Received in revised form
11 June 2016
Accepted 26 June 2016
Available online 29 June 2016

Keywords:
Nanoparticles
Antifouling paint
Copper
Environmental fate
Toxicity

ABSTRACT

One major concern with the use of antifouling paints is the release of its biocides (mainly copper and zinc) into natural waters, where they may exhibit toxicity to non-target organisms. While many studies have quantified the release of biocides from antifouling paints, very little is known about the physicochemical state of released copper. For proper risk assessment of antifouling paints, characterization of copper released into water is necessary because the physicochemical state determines the metal's environmental fate and effects. In this study, we monitored release of different fractions of copper (dissolved, nano, and bulk) from a commercial copper-based antifouling paint. Release from painted wood and aluminum mini-bars that were submerged in natural waters was monitored for 180 days. Leachates contained both dissolved and particulate copper species. X-ray diffraction and X-ray photoelectron spectroscopy were used to determine the chemical phase of particles in the leachate. The amount of copper released was strongly dependent on water salinity, painted surface, and paint drying time. The presence of nanosized Cu_2O particles was confirmed in paint and its leachate using single-particle inductively coupled plasma-mass spectrometry and electron microscopy. Toxicity of paint leachate to a marine phytoplankton was also evaluated.

1. Introduction

Fouling organisms are undesirable on hulls of ships and boats because they increase drag, and thus reduce fuel economy, and speed, and maneuverability of vessels (Kiil et al., 2001; Valkirs et al., 2003). Inorganic and organic copper (Cu) compounds have long been employed as biocidal agents, and have found use in antifouling (or bottom) paints to prevent colonization of vessel hulls by fouling organisms such as barnacles, tube worms, and algae (Omae, 2003; Turner, 2010). One major concern about the use of antifouling paint has to do with passive leaching of biocides into waters during use (Katranitsas et al., 2003; Warnken et al., 2004). Antifouling paint particles may also be released into aquatic systems when spent paint residues are removed during maintenance (Parks et al., 2010). Water and sediment quality surveys in harbors, marinas, and vessel maintenance facilities have found unusually high levels of Cu (Comber et al., 2002; Hall et al., 1988; Omae, 2003; Parks et al., 2010).

Several studies have investigated release of Cu from antifouling paints. For instance, Hall et al. (1988) monitored dissolved Cu in Chesapeake Bay for 11 months and concluded that recreational boats housed in a marina were most likely responsible for high levels of Cu detected. Comber et al. (2002) found that Cu concentration in summer months was twice as much as in winter in an estuary, which was largely attributed to leaching of antifouling paints biocides. Valkirs and coworkers detected dissolved Cu release rate into San Diego Bay of 8 $\mu g/cm^2$-day from hulls of US Navy vessels and 65 $\mu g/cm^2$-day from painted steel panels (Valkirs et al., 2003). In all these studies (and others), dissolved Cu was defined as the fraction < 0.45 μm, as is traditionally done. However, this classification of dissolved Cu lumps together dissolved ions, nanoparticles (generally defined as particles with at least one dimension between 1 and 100 nm) and some bulk particles (100–450 nm in size). For proper risk assessment, it is necessary to determine how much of these different fractions of Cu are leached from antifouling paints since their fate, bioavailability, and toxicity differ considerably (Bielmyer-Fraser et al., 2014; Shi et al., 2011;

* Corresponding author. Bren School of Environmental Science & Management, University of California, Santa Barbara, CA 93106-5131, USA.
E-mail address: keller@bren.ucsb.edu (A.A. Keller).

http://dx.doi.org/10.1016/j.watres.2016.06.056
0043-1354/

Siddiqui et al., 2015; Thit et al., 2013; Torres-Duarte et al., 2015).

The goal of this study was to investigate how (1) water salinity, (2) type of surface painted, and (3) consumer behavior (paint drying/curing time) affect the release of different size-fractions of Cu from a commercial antifouling paint. In addition, we investigated the chemical state of Cu particles found in water, which were either from undissolved particles or formed via precipitation. High throughput assays were carried out to test the effects of paint leachate on a marine phytoplankton.

2. Materials and methods

2.1. Antifouling paint particle characterization

A commercial self-polishing antifouling paint, Sea Hawk Cukote Biocide Plus Red-3541 (New Nautical Coatings, Clearwater, FL), was used for this study. According to the manufacturer, the antifouling paint has 47.57% Cu_2O as the main biocidal ingredient; this information was verified (details below). The composition of the antifouling paint as provided by the manufacturer is shown in Fig. A.1 (in Appendix A). Particles in paint were characterized via dynamic light scattering (DLS, Malvern Zetasizer Nano-ZS90), X-ray diffraction (XRD, Bruker D8 Advance), and scanning electron microscopy (SEM, FEI XL30 Sirion equipped with an EDAX APOLLO X probe for energy-dispersive X-ray spectroscopy, EDS). Stock for DLS measurement was prepared by diluting paint in deionized (DI) water (Barnstead NANOpure Diamond) by a factor of 100, and the emulsion was bath-sonicated (Branson 2510) for 1 h. 0.1 mL of the supernatant was then added to 0.9 mL DI water and analyzed using the Zetasizer. The amount of Cu in paint was determined by a combination of ultrasonication (Branson 8800) and acid digestion (Fisher Scientific trace-metal grade HNO_3) of diluted paint followed by ICP-MS analysis (Agilent 7900, Agilent Technologies, Santa Clara, CA). A graphical summary of the methodology is provided in Appendix A.

2.2. Single particle analysis using ICP-MS

Single particle inductively coupled plasma-mass spectrometry (sp-ICP-MS) was also employed to further characterize the paint using an Agilent 7900 ICP-MS (e.g. Yamanaka et al., 2015). Method setup and data analyses were done in the Single Nanoparticle Application Module ICP-MS MassHunter software (Agilent Technologies). Analyses were performed in time resolved analysis (TRA) mode using an integration time of 0.1 ms per point with no settling time between measurements. NIST 8012 Au reference material (nominal diameter = 30 nm) was employed for determination of nebulization efficiency. The reference material was diluted to 10 ng/L with 8% ethanol in DI and sonicated for 5 min to ensure homogeneity. A NIST-traceable Cu standard (diluted to 1 μg/L) was used to determine the elemental response factor. The paint was diluted with DI water (while sonicating) such that the Cu particle concentration was between 10 and 100 ng/L, and a sample inlet flow of 0.346 mL/min was used. Analyte mass fraction was set to 0.89 while particle density was set to 6 g/cm^3.

2.3. Painted surfaces and experimental set-up

Aluminum sheets (~2 mm thick, 5052 non-heat treatable alloy, Industrial Metal, Ventura, CA) and oak wood (American Wood Moulding, Hanover, MD) were used for this study. Wood was cut into 3 × 1 × 1 cm mini-bars while aluminum sheet was cut into 3 × 1 cm mini-bars. The aluminum and wood mini-bars were pretreated and painted in accordance with the manufacturer's instruction (see Section A.1.0 in the Appendix). Each mini-bar was weighed (Denver Instrument SI-114) after all surface treatments, before and after painting to determine mass of paint applied. Painted mini-bars were allowed to dry for 6 h, 24 h (minimum time recommended by paint manufacturer), or 7 d, and then submerged in water (20 mL of freshwater, estuary, or seawater). Estuary water was composed of 50% freshwater (laboratory tap water; dissolved organic carbon = 1.98 mg-C/L) and 50% seawater (collected from the Pacific Ocean in Santa Barbara and 0.2 μm-filtered). Filtration was done to remove potential interferences such as microorganisms, suspended sediments, and other debris. Characterization of seawater was provided in a previous study (Keller et al., 2010). Submerged coated mini-bars were kept in conditions simulating natural surface waters: cool white fluorescent lights (14:10 light:-dark, 80–100 μmol/m^2-s) at 20 °C with shaking (125 rpm) (Adeleye and Keller, 2014; Miller et al., 2012).

2.4. Biocide release studies

Release of Cu from wood and aluminum mini-bars was monitored as a time series for 180 d. Each mini-bar was sacrificed after analysis. Full description of the release monitoring is provided in Section A.2.0. Briefly, we analyzed for total Cu (Cu_{total}), dissolved Cu (Cu_{diss}), nanosized Cu (Cu_{nano}), and bulk Cu (Cu_{bulk}). Cu_{diss} was obtained using Millipore Amicon Ultra-4 3 kDa centrifugal filter tubes (maximum pore size ~ 2 nm) while Cu_{nano} was separated using Thermo Scientific Target2 PVDF 0.2 μm filters (preliminary analyses showed that nanoparticles in paint were 80–200 nm in diameter). Morphology and elemental composition of particles in leachates were studied via transmission electron microscopy (TEM) analyses using a Titan 300 kV FEG TEM/STEM microscope equipped with an Oxford INCA x-sight EDS probe.

2.5. Transformation of Cu biocides in waters

To study the transformation of Cu species released from the antifouling paint, 5 mL of antifouling paint were added to 45 mL of the three different waters. The individual mixtures were placed on a Dayton-6Z412A Parallel Shaft roller mixer (90 rpm), and analyzed at intervals for up to 180 d. To analyze, the dissolved phase was separated from solids via centrifugation (6000*g*, 30 min, Sorvall RC 5B Plus). The solid phase was then dried in a Baxter vacuum dryer and analyzed via X-ray photoelectron spectroscopy (XPS) and XRD to determine the chemical states of particulate Cu. XPS analyses were carried out with a Kratos Axis Ultra DLD spectrometer using a monochromatic Al Kα source at 225 W. Samples were spread over double-sided tape, and an analysis area of 300 μm × 700 μm was used. Instrument base pressure was below 10^{-8} Torr. All survey spectra were collected at 160 eV pass energy, 0.5 eV step, and 150 ms dwell time per sample. High-resolution spectra were collected using 20 eV pass energy, 0.05 eV step, and 300 ms dwell time. Repeated analyses done using the same sample area and similar parameters showed reduction from Cu(II) to Cu(I) so the high resolution spectra for Cu 2p were collected differently. Cu 2p high resolution peaks were collected from areas that were not previously exposed to X-rays and the acquisition time was limited to 60 s using 40 eV pass energy, 0.1 eV steps, and 400 ms dwell time. We confirmed from preliminary analyses that Cu $2p_{3/2}$ peak areas are twice those of Cu $2p_{1/2}$ peaks, and that all the peaks used to determine the speciation of Cu in the Cu $2p_{3/2}$ and Cu $2p_{1/2}$ are equally distant apart. As such the data used for this manuscript was only collected for Cu$2p_{3/2}$ peaks (940–928 eV) to minimize sample exposure to X-rays. We confirmed that our samples were not altered by these acquisition conditions. The Kratos charge neutralizer system was used for all analyses with charge neutralization being monitored using the C 1s signal for adventitious

carbon. Spectra were analyzed using CasaXPS software (Fairley and Carrick, 2005) (version 2.3.16).

2.6. Effect of paint leachates on marine phytoplankton

Toxicity of paint leachate in marine systems was evaluated using algal growth-inhibition assays. An axenic culture of *Isochrysis galbana* was obtained from the Provasoli-Guillard National Center for Marine Algae and Microbiota (Bigelow Laboratory for Ocean Sciences, East Boothbay, ME), and was maintained as described previously (Miller et al., 2012) (summarized in Section A.3.0). To provide inoculant for experiments, the phytoplankton was incubated in 50 mL of f/2 media for 6 days. For the experiments, the cultures were inoculated at an initial density of 2×10^4 cells/mL in a black 96-well microplate with clear-bottom (Corning Inc., Kennebunk, ME) containing 200 μL of exposure solution. Incubation was done under cool white fluorescent lights (15,000 lux, 14:10 light:dark) at 20 °C. Light intensity was monitored using a Traceable™ Dual-Range Light Meter (Fisher Scientific). Cultures were mixed constantly at 400 rpm with a Talboys 1000 MP microplate shaker (orbit = 3 mm). Cell densities were monitored every 24 h for 5 d by measuring fluorescence (BioTek Synergy H1) at excitation wavelength of 485 nm and emission wavelength of 685 nm. Only the seawater leachates obtained after 180 d were tested, and were diluted by a factor of 10. Five replicates were used for each condition. The average specific growth rate of the algae for the duration of exposure was calculated according to the following logistic equation:

$$\mu_{i-j} = \frac{\ln X_i - \ln X_j}{t_i - t_j} \left(day^{-1}\right) \quad (1)$$

where μ_{i-j} is the average specific growth rate from time i to j; X_i and X_j are the relative fluorescence at time i and j, respectively; and t_i and t_j are the initial time of exposure and final time of exposure, respectively. Percentage inhibition of growth was calculated as:

$$I = \frac{\mu_C - \mu_T}{\mu_C} \times 100 \quad (2)$$

where I is the percent inhibition in average specific growth rate; μ_C is the average specific growth rate in the control group, and μ_T is the average specific growth rate for the treatment.

3. Result and discussions

3.1. Characterization of paint particles

Preliminary analysis of antifouling paint particles was done via DLS analysis of paint emulsion to determine if colloids, and specifically nanomaterials, were present. DLS data was collected every 30 s for 12 h so as to obtain representative data. As shown in Fig. A.2, the antifouling paint contained nanosized particles with a modal diameter of ~220 nm. In general the hydrodynamic diameter of nanomaterials is much greater than their primary particle size due to aggregation in aqueous phase, and the presence of water films around the particles (Adeleye et al., 2014). Therefore, the average primary particle size of the nanomaterials in the antifouling paint is probably less than 220 nm. Particles with hydrodynamic diameters ranging from 44 nm to 5 μm were detected by DLS analyses (Fig. A.2a). This agrees very well with (1) SEM analyses, shown in Fig. 1, where both nano- and micron-sized Cu particles were detected and confirmed via EDS hypermapping; and (2) sp-ICP-MS analyses, presented in Fig. 2, which shows that the most abundant particle size was 44 nm. As can be seen in the size distribution of the Cu particles in paint (Fig. 2), most of the particles analyzed were between 40 and 200 nm, although some low intensity peaks were observed up to 460 nm. The micron-sized particles shown via SEM analyses to be present in paint probably settled out of solution and were not detected during sp-ICP-MS analyses.

XRD analysis confirmed that the form of Cu in the antifouling paint is mainly cubic synthetic cuprite or Cu_2O (Fig. A.3), which agrees well with information from the manufacturer. ICP-MS analyses revealed that Cu concentration was 55.5% by mass. This is somewhat higher than the Cu content reported by the manufacturer (48%), and was used for all the calculations in this study.

3.2. Release of Cu from paint

3.2.1. Effect of painted material on Cu release

To quantify release of biocide from painted surfaces, we analyzed for Cu species the waters in which the mini-bars were submerged. The data presented and discussed in this section were derived from mini-bars dried for 24 h, and exposed in seawater; the effects of drying time and salinity are discussed later. The amount of Cu release increased over time: Cu concentration (in mg/L) increased from 0.01 to 41.5 and 1.47 to 625.7 between Days 0 and 180 in aluminum and wood mini-bars, respectively (Figs. 3 and A.4). In general, the mass of Cu found in leachates of wood mini-bar treatments was an order of magnitude (or more) higher than in corresponding aluminum treatments. This is partly due to the presence of higher amounts of antifouling paint on wood mini-bars and much higher release rate of antifouling paint (biocide) from wood. While their length and width were similar, wood mini-bars were 80% thicker than aluminum mini-bars. In addition, wood mini-bars were covered with three coats of the antifouling paint

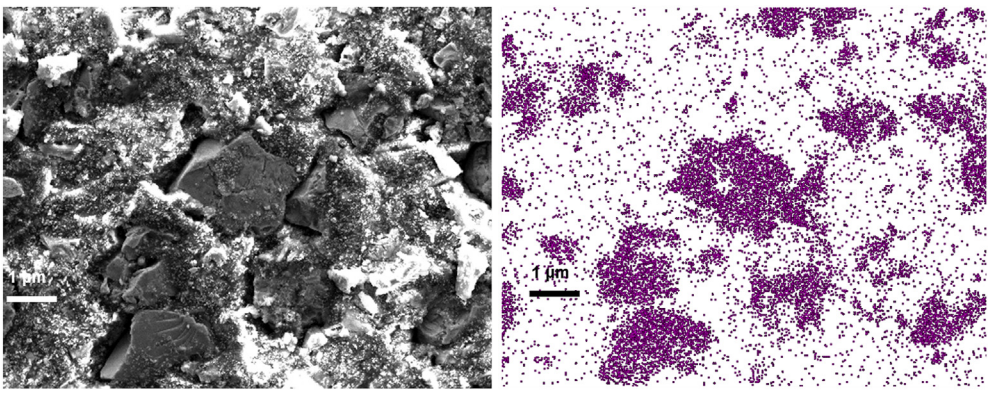

Fig. 1. Scanning electron micrograph of dried paint (left) and hypermap of copper in the sample (right) obtained from energy-dispersive X-ray spectroscopy (EDS) analysis.

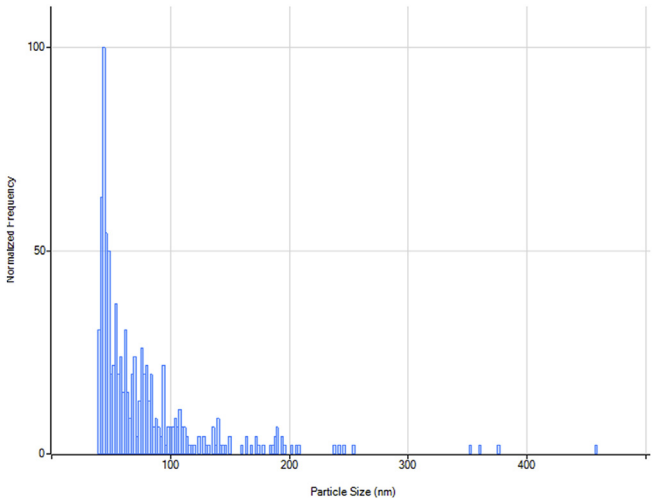

Fig. 2. Particle size distribution of Cu_2O (as Cu) present in antifouling paint obtained from single particle-ICP-MS.

versus two coats for aluminum (the minimum amount of coats suggested for the different surfaces by the manufacturer). To take into account the effect of higher amounts of antifouling paint on wood mini-bars (due to larger size and additional coating), the mass of Cu released from each mini-bar was normalized by the mass of Cu in their individual coatings. We found that maximum Cu released over 180 d was 0.21% from aluminum and 1.76% from wood. This result confirms that considerably more Cu was released from painted wood than aluminum surfaces.

Mass flux (F_{mass}) of Cu released from the mini-bars was derived by normalizing the mass of paint released over 180 d by the surface area of the mini-bars. F_{mass} was 3.01 μg/cm^2-day for aluminum mini-bars and 26.4 μg/cm^2-day for wood mini-bars in seawater. Release of biocides from surfaces painted with antifouling paints is controlled by biocide chemistry, hydrodynamics, temperature, salinity, pH, microbial biofilm (Kiil et al., 2001, 2002; Valkirs et al., 2003), and as shown here, painted material. When the mini-bars were removed from waters for sampling, we observed slight swelling of wood mini-bars. This suggests that wood mini-bars imbibed some water. In addition to swelling, we also observed cracks and peels on the antifouling paint coats of wood mini-bars (but not in aluminum mini-bars) that were submerged for a long time. This led us to believe that in addition to the leaching of biocides into water from antifouling paints, Cu was also released due to water percolating into the wood and the poor dimensional stability of wood in water, which is probably responsible for higher leachate amounts. It should be noted that such material instability may be less pronounced in real wooden hulls, which are typically made with much larger and thicker woods. The resins in antifouling paints are porous, allowing some inflow of water. Additionally some of the organic solvent in antifouling paints vaporized when the painted mini-bars were dried/cured and additional solvents may have been released into water when submerged, thereby reducing the hydrophobicity of the paint and allowing for penetration of water.

Unlike wood, the layers of epoxy primers on aluminum mini-bars (see Section A.1.0) effectively excluded water, and release was assumed to be due only to regular biocide leaching, as would be expected in any stable hull material. Although wooden hulls are becoming less popular, many sailboats and older ships have wooden hulls. As shown in this study, these types of hulls have the tendency to release a higher amount of biocides into surface waters than aluminum hulls. Other materials such as fiberglass and steel are often coated with impermeable epoxy primers prior to antifouling paint application, and are thus expected to behave similar to aluminum mini-bars used in this study. In fact, the release rate we found in aluminum mini-bars (3.01 μg/cm^2-day) is very similar to the mean in-situ release rate of Cu from the hull of US Naval vessels measured in San Diego Bay (3.8 μg/cm^2-day) (Valkirs et al., 2003).

3.2.2. *Effect of salinity on Cu release*

The amount of Cu detected in the aqueous phase over 180 d increased with increasing salinity (Figs. 3 and A.4). Cu_{total} from aluminum mini-bars (dried for 24 h) on day 180 was 4.47, 19.5, and 41.5 mg/L in DI, estuary, and seawater, respectively. Similarly, Cu_{total} from wood mini-bars at the same time period was 38.2, 243, and 626 mg/L in DI, estuary, and seawater, respectively. In addition to effects of salinity on the amount of Cu leached out of the mini-bars, a clear effect of salinity on the size fractions of released Cu was also observed. For instance, more than 90% of Cu_{total} detected within 2 h of exposing aluminum mini-bars to seawater was ionic Cu (Cu_{diss}); Cu_{nano} accounted for 7% while no bulk Cu was detected (Fig. 4). Cu_{diss} decreased gradually with time, but remained the predominant fraction for the first 7 days. Conversely, Cu_{bulk} increased steadily with time and was approximately equal to Cu_{diss} on day 14 after which it became the dominant fraction. The range of Cu_{nano} detected in seawater over 180 d was 1.5–7460 μg/L or 5–21% of Cu_{total}.

In contrast to our observations in seawater treatments, Cu_{diss} was either completely absent or only present at low levels within the first 7 days of exposing painted mini-bars to freshwater (Fig. 4). The fraction of Cu_{bulk} over the 180-d experiment period was 21–100%, making it the most predominant form in this low salinity medium. Cu_{nano} was as high as 38% of Cu_{total} within the first two weeks, after which it decreased steadily to 12%. The actual amount

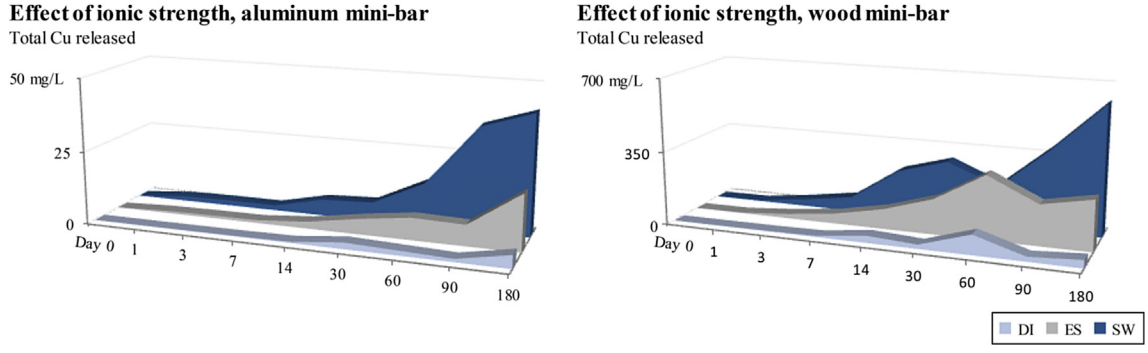

Fig. 3. Total Cu released from aluminum and wood mini-bars over 180 d. Freshwater = DI, estuary = ES, and seawater = SW. Paint drying time = 24 h.

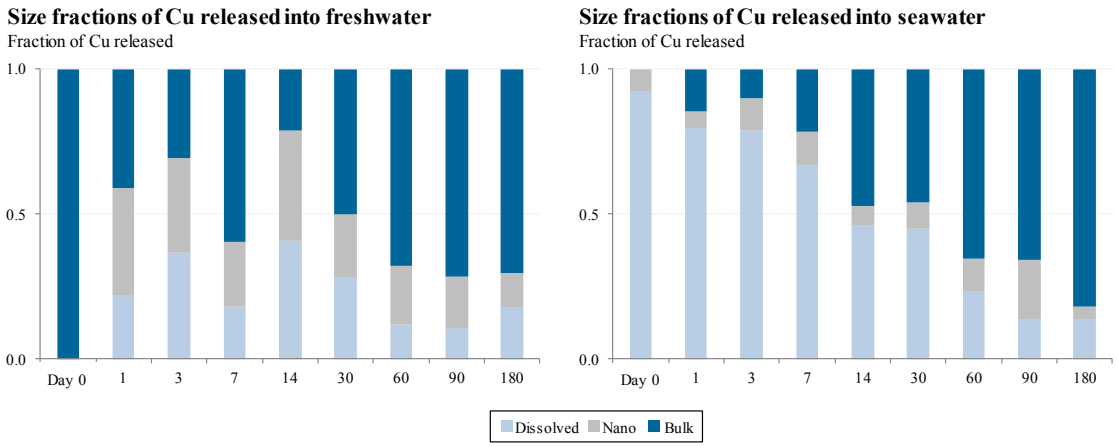

Fig. 4. Effect of ionic strength on size fractions of Cu released from aluminum mini-bars over 180 d. Paint drying time = 24 h.

of Cu_{nano} determined in freshwater during the experiment was 0–540 μg/L. There was no clear pattern in estuarine conditions (Fig. A.5) since it is a complex balance between freshwater and marine processes, but Cu_{diss} was the predominant Cu fraction, accounting for 28–88% of Cu_{total} over 180 d. Unlike the seawater treatments however, Cu_{bulk} did not become dominant throughout the 180-d period; and the fraction of Cu_{nano} was higher than in seawater but less than in freshwater (up to 32%).

The dissolution of Cu_2O in natural waters is largely controlled by the ions present, especially chloride (Cl^-) ions as shown in Eq. (3) (Ferry and Carritt, 1946; Singh and Turner, 2009). It is noteworthy that dissolution of Cu_2O may still occur when Cl^- is unavailable. In the absence of Cl^-, protons (H^+) may react with the oxygen (O) atom in Cu_2O to produce cuprous ions (Cu^+). However, the reaction rate is very slow at typical natural water pH range (~pH 6–8) (Ferry and Carritt, 1946). When antifouling paint-coated boat hulls are in water, Cu_2O particles in the paint matrix undergo a complexation reaction with Cl^-, releasing complexed Cu^+ into water (Eqs. (3) and (4)) (Ferry and Carritt, 1946; Kiil et al., 2001; Singh and Turner, 2009). In oxygenated water, Cu^+ may be rapidly converted to cupric ion (Cu^{2+}) (Adeleye et al., 2014; Kiil et al., 2001; Valkirs et al., 2003).

$$0.5Cu_2O + H^+ + 2Cl^- \leftrightarrow CuCl_2^- + 0.5H_2O \quad (3)$$

$$CuCl_2^- + Cl^- \leftrightarrow CuCl_3^{2-} \quad (4)$$

This explains the abundance of Cu_{diss} in seawater ($Cl^- \approx 19.3$ g/L (Keller et al., 2010)) and estuary ($Cl^- \approx 9.70$ g/L, based on dilution of seawater), compared to freshwater, ($Cl^- = 0.06$ g/L; determined by a $Hg(NO_3)_2$ titration method, Hanna Instruments) (Conway et al., 2015). Although the fraction of Cu_{diss} decreased over time in seawater, the actual concentration of Cu_{diss} increased from 18.4 μg/L at the start of the experiment to 555 μg/L after 180 d. Increasing amounts of Cu_{bulk} over time in seawater is probably due to the formation of Cu^{2+} solids (e.g. CuO, $Cu(OH)_2$ or $CuCl_2$, etc. as explained in Section 3.3) from oxidation of Cu^+ in bulk seawater and estuary. A low amount of Cl^- in freshwater explains the relatively low Cu_{diss} and overall leaching rate of Cu from the antifouling paint in that condition (Figs. 3 and A.4). In fact, our results show a clear linear relationship between Cl^- concentration and Cu release rate ($R^2 = 0.999$ in wood and 0.981 in aluminum, Fig. A.6).

In general, dissolved organic carbon (DOC) enhances dissolution of Cu in natural waters via complexation (Adeleye et al., 2014; Conway et al., 2015). In this study however, complexation of Cu by DOC is minimal compared to that of Cl^- based on the amounts of both complexing agents present. The DOC in the tap water used in this study (1.98 mg-C/L) is thrice as much as that in the seawater (0.65 mg-C/L). As such, increased dissolution of Cu in seawater is mainly due to Cl-complexation and not DOC complexation.

3.2.3. *Effect of drying time on Cu release*

In addition to mini-bars coated with the antifouling paint and dried for 24 h (as recommended by the paint manufacturer), additional mini-bars were coated with the antifouling paint and dried for 3 h (short drying time) or 7 d (long drying time) in other to see how consumer behavior may influence leaching of Cu from antifouling paints. As shown in Fig. 5, mass of Cu released over 180 d increased with paint drying time, which is counterintuitive.

In general, as oil-based paints dry out (cure) many of the organics in the paint volatilize while the polymers, pigments and other additives harden. These processes increase the porosity of the paint matrix, while somewhat also reducing its hydrophobicity. As a result, more water is able to percolate into the paint matrix with increased drying time, leading to increased Cu_2O dissolution and leaching. The effect of drying time was stronger in wood mini-bars compared to aluminum mini-bars (Fig. 5). This is in agreement with our earlier observation that increased leaching of Cu from wood mini-bars is partly due to imbibition of water by the mini-bars. This suggests that a painted boat should be placed back in water shortly after the manufacturer's specified curing time, particularly if it is wooden.

In general, our results demonstrate that release of biocides from antifouling paints is influenced by consumer behavior. As shown here, allowing painted hulls to dry for much longer than recommended by the antifouling paint manufacturer may actually lead to additional release of biocides into water. In addition, the type of surface on which antifouling coatings are applied influences leaching of biocides, as materials with poor dimensional stability such as wood may lead to additional leaching.

3.3. *Transformation of released Cu*

XRD and XPS analyses were used to characterize the particulate materials in leachates of paint in order to better understand how Cu_2O particles in the antifouling paint are transformed over time in natural waters. A combination of these two X-ray techniques is extremely useful for probing transformation at particle surface since XPS determines surface composition to a depth of 8–12 nm while XRD can penetrate up to hundreds of microns into particles.

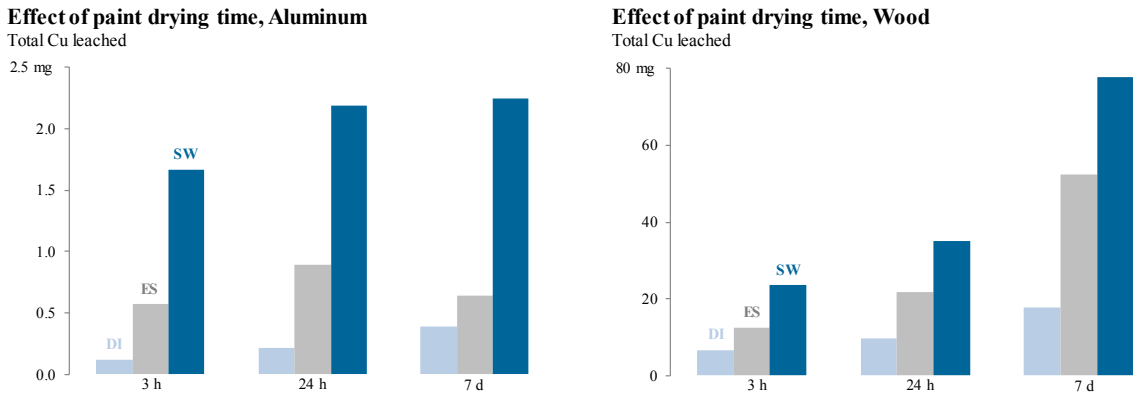

Fig. 5. Effect of paint drying time (3 h, 24 h, and 7 d) on mass of Cu released from aluminum and wood mini-bars into freshwater (DI), estuary (ES), and seawater (SW) over 180 d. Note the difference in y-axis scales.

The dominant peaks detected in XRD diffractograms in all three waters (up to 180 d) were assigned to Cu_2O, although major peaks for ZnO and Fe_2O_3 were also detected (Fig. A.7). Other chemical states of Cu observed in the XRD data were CuCl ($2\theta \approx 29.0°$), and $CuCl_2$ ($2\theta \approx 45.9°$), which were only detected in seawater samples. Also, a peak for $CuCl_2$ was only observed in Day 180 samples. These results suggest that the environmental transformation of Cu_2O embedded in the antifouling paint used in this study is quite slow—taking weeks to months. In addition, precipitation of dissolved Cu ions in marine systems is driven by Cl^-, which is also mainly responsible for Cu dissolution, as discussed earlier.

For XPS analyses, all of the peaks used to model different Cu species have full width at half maximum (FWHM) values that are ± 0.3 eV (instead of the more conventional ± 0.2 eV) due to the complexity of the paint matrix and the low resolution of the data that was necessitated by Cu(II) alteration by X-rays. XPS survey scans of the particulate paint materials showed an abundance of C and O atoms (Fig. A.8), which are probably from the polymers, hydrocarbons, and resins in the paint matrix (Fig. A.1). In addition, zinc, silicon, and magnesium were detected, which were also listed as ingredients by the manufacturer. Although about half of the paint mass is Cu, the amount of Cu detected by XPS was relatively low. This is mainly because Cu particles in self-polishing antifouling paints are typically encapsulated in resins within the paint matrix. Encapsulation is done to control the release/transformation of Cu, and was visualized in this study via SEM analysis (Fig. 1).

High resolution XPS analyses of samples obtained after 180 d are shown in Figs. 6 and A.9. The abundance of Cu(II) species was much higher than Cu(I) in the samples exposed to marine conditions while Cu(I) was more abundant in freshwater samples, showing the effect of salinity in the transformation of Cu_2O in antifouling paints. Deconvolution of the high resolution scans of Cu $2p_{3/2}$ peaks (Figs. 6b and A.9) revealed that Cu was present as Cu_2O in samples obtained from all three media (BE ≈ 932.2 eV) (Moulder et al., 1995), which agrees with the XRD analyses. The peaks found around 934.1 eV in samples from all three waters may be assigned to CuO, $CuCO_3(OH)_2$, and $CuCl_2$ (Dzhurinskii et al., 1975; Moulder et al., 1995; Vasquez, 1998). Since we did not detect the C 1s peak for carbonate (typically at 289.1 eV (Vasquez, 1998), Fig. A.10), we assigned the peak to CuO and $CuCl_2$, which also agrees with XRD analysis. The peak at 935.2 eV was assigned to $Cu(OH)_2$ (Dake et al., 2000; Moulder et al., 1995). While the fraction of Cu_2O in the Cu $2p_{3/2}$ peaks was relatively constant over time in the samples obtained from freshwater, it decreased progressively over time in the marine water-exposed samples. For instance, Cu_2O fraction was 65%, 47%, and 29% in samples exposed to seawater for 2 h, 30 d, and 180 d, respectively (data not shown). These X-ray data show that Cu_2O particles in the antifouling paint are progressively transformed into CuO or $CuCl_2$ while dissolved Cu is precipitated as $Cu(OH)_2$ especially in marine waters. This agrees well with our finding of dominance of bulk Cu– over time –in the seawater treatments (Fig. 4). In a previous study using MINTEQ modeling, copper nanoparticles were predicted to oxidize, at equilibrium, mainly to CuO and $Cu_2Cl(OH)_3$ in marine systems (Conway et al., 2015). It should be noted that CuO can also dissolve to an extent over time, leading to more complexation and precipitation

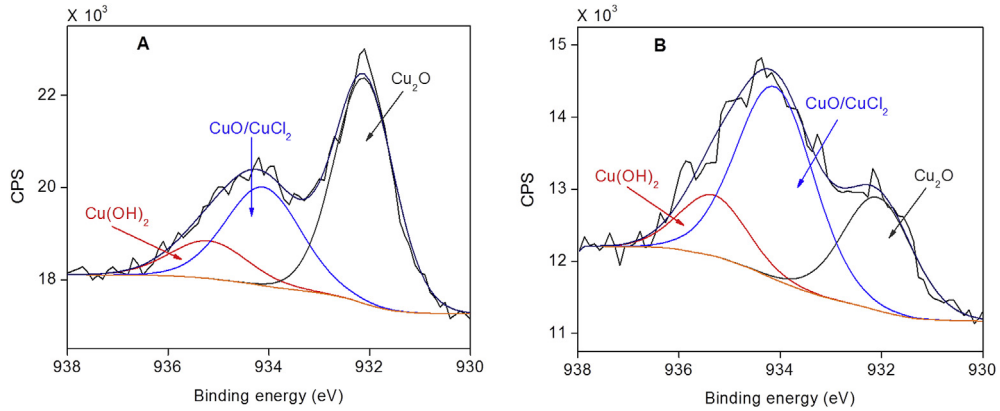

Fig. 6. High resolution Cu $2p_{3/2}$ spectra of solid fractions of antifouling paint obtained after 180 d of immersion in (A) freshwater and (B) seawater showing the difference in the abundance of Cu(I) and Cu(II) species. Sample acquisition time was minimized to prevent sample alteration by X-ray.

(Adeleye et al., 2014; Conway et al., 2015).

A TEM micrograph of paint leachate showing the presence of particles is shown in Fig. 7. Particles in the leachates range in size from the nanoscale to a few microns. EDS analyses confirmed that the particles were composed mainly of Cu and O, most likely Cu_2O as indicated by XRD and XPS. The other elements detected by EDS (C, Cl) may be from the TEM grid and/or aqueous media. The size of Cu_2O particles is very important for the behavior of antifouling paints as smaller particles significantly increase polishing/leaching (Kiil et al., 2002). The environmental implications of these nano-sized particles may also be different from that of bulk materials. It has been shown that smaller sized Cu particles tend to dissolve faster, and exhibit a higher toxic effect to aquatic organisms (Cai et al., 2005; Torres-Duarte et al., 2015).

The TEM with EDS data, which were obtained from samples submerged for 180 d, further proves that transformation of Cu_2O in the antifouling paint is not very rapid. It is noteworthy that the transformation rate of Cu_2O particles in water may have been decreased due to saturation under the study conditions. In addition, self-polishing paints are designed to slowly release their biocides over time as water erodes the active polymer through hydrolysis (self-polishing effect) (Kiil et al., 2002). As such, the particles detected after 180 d of paint exposure may have only been released into water for a much shorter time.

3.4. Effect of paint leachates on marine phytoplankton

The paint leachates obtained after submerging the mini-bars in seawater for 180 d were exposed to *I. galbana* (a marine phytoplankton) in order to evaluate the potential effects of paint leachates in marine systems. Phytoplankton are primary producers in aquatic systems, and have long being used to evaluate the environmental impacts of chemicals; phytoplankton are not a primary target of the biocide in these paints. The leachates were diluted by a factor of 10 with pristine seawater prior to exposure in order to reduce the concentrations of Cu, and to simulate the concentration at a distance away from the immediate surface. Each diluted leachate was exposed to phytoplankton (at an initial density of 2×10^4 cells/mL) and growth inhibition over 5 d was used as toxicity endpoint. Inhibition greater than 100% implies cell death.

The paint leachates significantly inhibited the growth of *I. galbana* ($p < 0.004$) as shown in Fig. 8. Inhibition of growth was more severe when the phytoplankton were exposed to leachates obtained from wood mini-bars (inhibition = 144–207%) than those obtained from aluminum mini-bars (50–133%). This agrees with the trend of Cu concentration we detected in the leachates, which was much higher in the wood mini-bar treatments. There was however no clear correlation between percent inhibition and paint drying time. The other non-Cu biocides present in the antifouling paint (e.g. ZnO, irgarol, etc.; Fig. A.1), which we did not account for in this study, may have complicated the toxicity pattern we observed (Dahl and Blanck, 1996).

4. Conclusions and environmental implications

Cu_2O particles in commercial antifouling paints may be released into natural waters during use. These released particles may include those that are nanoparticulate in size. The size of Cu_2O particles is very important for the behavior of antifouling paints as smaller particles significantly increase polishing/leaching (Kiil et al., 2002). The environmental implications of these nanosized particles may also be different from that of bulk materials. It has

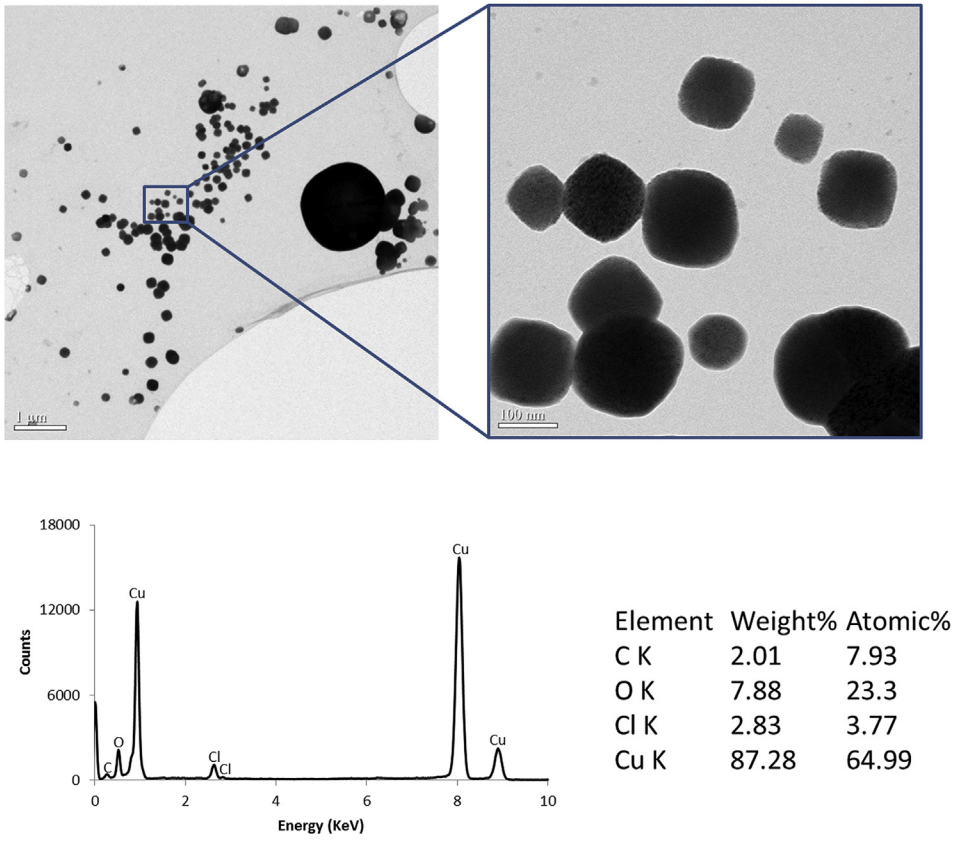

Fig. 7. TEM micrographs and EDS analyses of particles detected in paint leachate. Leachate was collected from aluminum mini-bars submerged in seawater for 180 d.

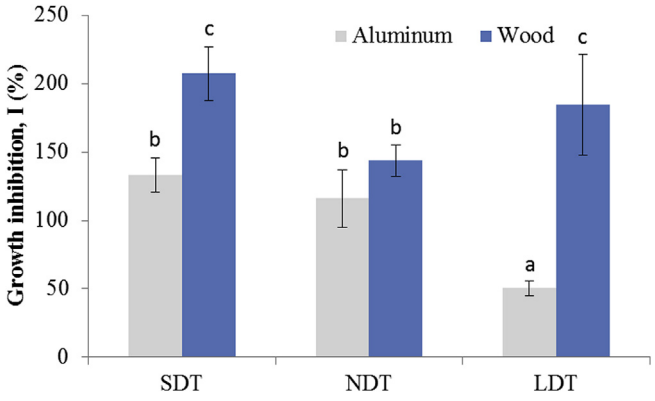

Fig. 8. Growth inhibition of *Isochrysis galbana* after a 5 d exposure to paint leachates from aluminum and wood mini-bars that were submerged in natural seawater for 180 d. Mini-bars were dried for 6 h (short drying time or SDT), 24 h (normal drying time or NDT), or 7d (long drying time or LDT) prior to submerging them in seawater. Leachates were diluted by a factor of 10 prior to exposure experiments. Mean values represented by distinct letters indicate significant differences detected by one-way ANOVA followed by posthoc Tukey's test.

been shown that smaller sized Cu particles tend to dissolve faster, and exhibit a higher toxic effect to aquatic organisms (Cai et al., 2005; Torres-Duarte et al., 2015).

Release of biocides from surfaces painted with antifouling paints is controlled mainly by biocide chemistry and environmental factors. However, release of biocides from antifouling paints may also be influenced by consumer behavior. As shown here, allowing painted hulls to dry for much longer than recommended by the antifouling paint manufacturer may actually lead to additional release of biocides into water. In addition, the type of surface on which antifouling coatings are applied influences leaching of biocides, as materials with poor dimensional stability such as wood may lead to additional leaching.

In addition to pH, the dissolution and transformation of Cu_2O particles in natural waters (where pH range is quite narrow) is mainly driven by Cl^- concentrations, which is abundant in marine systems. However, although saturation is not likely in natural waters (at least, over time), the transformation rate of Cu_2O particles released into natural waters from antifouling paints will decrease due to their encapsulation in resins. As a result, persistence of these potentially reactive metals in the environment will increase, especially in freshwater systems. Although environmental transformation may increasingly lead to complexation of Cu (and thus, reduced bioavailability), the leachates may still pose significant threat to important ecological species.

This study investigated the physicochemical state of the biocides present in the leachate of a Cu_2O-based antifouling paint. In summary, we found that:

- There were nanosized Cu_2O particles in the commercial antifouling paint (in addition to micronsized Cu_2O), although the paint was not labeled as nano-enabled. Nanosized Cu was also detected in the leachates of the commercial paint over 180 days;
- In natural waters, dissolution and leaching of Cu_2O in the paint is driven mainly by Cl^- concentrations, leading to very high release of both dissolved and particulate Cu into seawater compared to freshwater;
- X-ray analyses showed that Cu_2O particles in the antifouling paint were progressively transformed into CuO while dissolved Cu is precipitated as $CuCl_2$, $Cu(OH)_2$. Despite the complexation, however, paint leachate was very toxic to marine phytoplankton; and
- Length of paint drying time and type of surface painted strongly influenced the amount of Cu released from antifouling paint into natural waters.

Acknowledgement

This material is based upon work supported by the National Science Foundation (NSF) and the Environmental Protection Agency (EPA) under Cooperative Agreement Number DBI 0830117. Any opinions, findings, and conclusions or recommendations expressed in this material are those of the authors and do not necessarily reflect the views of NSF or EPA. This work has not been subjected to EPA review and no official endorsement should be inferred. We thank the MRL Central Facilities, which are supported by the MRSEC Program of the NSF under Award No. DMR 1121053. The authors also thank Sage Davis for helping with mini-bar preparation, and Oluwaseun Sodimu and Edward Hadeler for their help with painting the mini-bars. We also appreciate Agilent Technologies for the Agilent Thought Leader Award given to A.A.K and the anonymous reviewers for their valuable contributions.

Appendix A. Supplementary data

Supplementary data related to this article can be found at http://dx.doi.org/10.1016/j.watres.2016.06.056.

References

Adeleye, A.S., Conway, J.R., Perez, T., Rutten, P., Keller, A.A., 2014. Influence of extracellular polymeric substances on the long-term fate, dissolution, and speciation of copper-based nanoparticles. Environ. Sci. Technol. 48 (21), 12561–12568.
Adeleye, A.S., Keller, A.A., 2014. Long-term colloidal stability and metal leaching of single wall carbon nanotubes: effect of temperature and extracellular polymeric substances. Water Res. 49 (0), 236–250.
Bielmyer-Fraser, G.K., Jarvis, T.A., Lenihan, H.S., Miller, R.J., 2014. Cellular partitioning of nanoparticulate versus dissolved metals in marine phytoplankton. Environ. Sci. Technol. 48 (22), 13443–13450.
Cai, S., Xia, X., Xie, C., 2005. Research on Cu2+ transformations of Cu and its oxides particles with different sizes in the simulated uterine solution. Corros. Sci. 47 (4), 1039–1047.
Comber, S.D.W., Gardner, M.J., Boxall, A.B.A., 2002. Survey of four marine antifoulant constituents (copper, zinc, diuron and Irgarol 1051) in two UK estuaries. J. Environ. Monit. 4 (3), 417–425.
Conway, J.R., Adeleye, A.S., Gardea-Torresdey, J., Keller, A.A., 2015. Aggregation, dissolution, and transformation of copper nanoparticles in natural waters. Environ. Sci. Technol. 49 (5), 2749–2756.
Dahl, B., Blanck, H., 1996. Toxic effects of the antifouling agent irgarol 1051 on periphyton communities in coastal water microcosms. Mar. Pollut. Bull. 32 (4), 342–350.
Dake, L.S., King, D.E., Czanderna, A.W., 2000. Ion scattering and X-ray photoelectron spectroscopy of copper overlayers vacuum deposited onto mercaptohexadecanoic acid self-assembled monolayers. Solid State Sci. 2 (8), 781–789.
Dzhurinskii, B., Gati, D., Sergushin, N., Nefedov, V., Salyn, Y.V., 1975. Simple and coordination compounds. An X-ray photoelectron spectroscopic study of certain oxides. Russ. J. Inorg. Chem. 20, 2307–2314.
Fairley, N., Carrick, A., 2005. The Casa Cookbook—part 1: Recipes for XPS Data Processing, Knutsford. Acolyte Science.
Ferry, J.D., Carritt, D.E., 1946. Action of antifouling paints - Solubility and rate of solution of cuprous oxide in sea water. Ind. Eng. Chem. 38 (6), 612–617.
Hall, W.S., Bushong, S., Hall Jr., L., Lenkevich, M., Pinkney, A., 1988. Monitoring dissolved copper concentrations in Chesapeake Bay, U.S.A. Environ. Monit. Assess. 11 (1), 33–42.
Katranitsas, A., Castritsi-Catharios, J., Persoone, G., 2003. The effects of a copper-based antifouling paint on mortality and enzymatic activity of a non-target marine organism. Mar. Pollut. Bull. 46 (11), 1491–1494.
Keller, A.A., Wang, H., Zhou, D., Lenihan, H.S., Cherr, G., Cardinale, B.J., Miller, R., Ji, Z., 2010. Stability and aggregation of metal oxide nanoparticles in natural aqueous matrices. Environ. Sci. Technol. 44 (6), 1962–1967.
Kiil, S., Weinell, C.E., Pedersen, M.S., Dam-Johansen, K., 2001. Analysis of self-polishing antifouling paints using rotary experiments and mathematical modeling. Ind. Eng. Chem. Res. 40 (18), 3906–3920.
Kiil, S., Weinell, C.E., Pedersen, M.S., Dam-Johansen, K., 2002. Mathematical modelling of a Self-polishing antifouling paint exposed to seawater: a parameter study. Chem. Eng. Res. Des. 80 (1), 45–52.
Miller, R.J., Bennett, S., Keller, A.A., Pease, S., Lenihan, H.S., 2012. TiO_2 nanoparticles

are phototoxic to marine phytoplankton. PloS One 7 (1), e30321.
Moulder, J., Stickle, W., Sobol, P.E., Bomben, K., 1995. Handbook of X-ray Photoelectron Spectroscopy. A Reference Book of Standard Spectra for Identification and Interpretation of Xps Data. Physical Electronics, Minnesota, USA.
Omae, I., 2003. General aspects of tin-free antifouling paints. Chem. Rev. 103 (9), 3431–3448.
Parks, R., Donnier-Marechal, M., Frickers, P.E., Turner, A., Readman, J.W., 2010. Antifouling biocides in discarded marine paint particles. Mar. Pollut. Bull. 60 (8), 1226–1230.
Shi, J., Abid, A.D., Kennedy, I.M., Hristova, K.R., Silk, W.K., 2011. To duckweeds (Landoltia punctata), nanoparticulate copper oxide is more inhibitory than the soluble copper in the bulk solution. Environ. Pollut. 159 (5), 1277–1282.
Siddiqui, S., Goddard, R.H., Bielmyer-Fraser, G.K., 2015. Comparative effects of dissolved copper and copper oxide nanoparticle exposure to the sea anemone, *Exaiptasia pallida*. Aquat. Toxicol. 160, 205–213.
Singh, N., Turner, A., 2009. Leaching of copper and zinc from spent antifouling paint particles. Environ. Pollut. 157 (2), 371–376.
Thit, A., Selck, H., Bjerregaard, H.F., 2013. Toxicity of CuO nanoparticles and Cu ions to tight epithelial cells from Xenopus laevis (A6): effects on proliferation, cell cycle progression and cell death. Toxicol. Vitro 27 (5), 1596–1601.
Torres-Duarte, C., Adeleye, A.S., Pokhrel, S., Mädler, L., Keller, A.A., Cherr, G.N., 2015. Developmental effects of two different copper oxide nanomaterials in sea urchin (*Lytechinus pictus*) embryos. Nanotoxicology 1–9.
Turner, A., 2010. Marine pollution from antifouling paint particles. Mar. Pollut. Bull. 60 (2), 159–171.
Valkirs, A.O., Seligman, P.F., Haslbeck, E., Caso, J.S., 2003. Measurement of copper release rates from antifouling paint under laboratory and in situ conditions: implications for loading estimation to marine water bodies. Mar. Pollut. Bull. 46 (6), 763–779.
Vasquez, R.P., 1998. CuCO3 by XPS. Surf. Sci. Spectra 5 (4), 273–278.
Warnken, J., Dunn, R.J.K., Teasdale, P.R., 2004. Investigation of recreational boats as a source of copper at anchorage sites using time-integrated diffusive gradients in thin film and sediment measurements. Mar. Pollut. Bull. 49 (9–10), 833–843.
Yamanaka, M., Yamanaka, K., Itagaki, T., 2015. Automated, High Sensitivity Analysis of Single Nanoparticles Using the Agilent 7900 ICP-MS with Single Nanoparticle Application Module. Agilent Technologies, pp. 1–5.